Original Article

Early evaluation of subclinical cardiotoxicity in patients with lung cancer receiving immune checkpoint inhibitors by cardiovascular magnetic resonance: a prospective observational study

Jia Liu[1,2], Yukun Cao[1,2], Kuikui Zhu[3], Sheng Yao[4], Mei Yuan[1,2], Xiangchuang Kong[1,2], Xiaoming Liu[1,2], Yumin Li[1,2], Yue Cui[1,2], Xiaoyu Han[1,2], Xiaoyue Zhou[5], Rui Meng[3#], Heshui Shi[1,2#]

[1]Department of Radiology, Union Hospital, Tongji Medical College, Huazhong University of Science and Technology, Wuhan, China; [2]Hubei Province Key Laboratory of Molecular Imaging, Wuhan, China; [3]Cancer Center, Union Hospital, Tongji Medical College, Huazhong University of Science and Technology, Wuhan, China; [4]Department of Rehabilitation Medicine, Tongji Hospital, Tongji Medical College, Huazhong University of Science and Technology, Wuhan, China; [5]MR Collaboration, Siemens Healthineers Ltd., Shanghai, China

Contributions: (I) Conception and design: H Shi, R Meng, J Liu; (II) Administrative support: H Shi, X Kong, X Liu; (III) Provision of study materials or patients: R Meng, J Liu, K Zhu; (IV) Collection and assembly of data: J Liu, M Yuan, X Zhou; (V) Data analysis and interpretation: J Liu, Y Cao, S Yao, Y Cui, Y Li, X Han; (VI) Manuscript writing: All authors; (VII) Final approval of manuscript: All authors.

[#]These authors contributed equally to this work.

Correspondence to: Heshui Shi. Department of Radiology, Union Hospital, Tongji Medical College, Huazhong University of Science and Technology, 1277 Jiefang Avenue, Wuhan 430022, China. Email: heshuishi@hust.edu.cn; Rui Meng. Cancer Center, Union Hospital, Tongji Medical College, Huazhong University of Science and Technology, 1277 Jiefang Avenue, Wuhan 430022, China. Email: mengruivip@163.com.

Background: Few studies have focused on the subclinical cardiotoxicity of immune checkpoint inhibitors (ICIs) in cancer patients. This study aimed to evaluate the manifestations of subclinical cardiotoxicity of ICI therapy using cardiovascular magnetic resonance (CMR) and to explore whether CMR parameters can help predict cardiotoxicity at the early stage of ICI therapy.

Methods: A prospective, longitudinal study was conducted among patients with lung cancer. The patients were planned to undergo serial CMRs before (baseline), 3 weeks after (1st follow-up), and 3 months after (2nd follow-up) the initiation of ICI therapy, respectively. Patients with 3 CMRs were included in the analysis. Serial quantitative measurements based on CMR were compared using one-way repeated measures analysis of variance (RM-ANOVA). On the basis of cancer therapy-related cardiac dysfunction (CTRCD) observed at the second follow-up, patients were categorized into a CTRCD group and a non-CTRCD group. Baseline clinical and CMR parameters and the relative reduction of left ventricular global strain at the second follow-up was compared between the CTRCD group and the non-CTRCD group. Receiver operating characteristic (ROC) analysis was used to identify CTRCD that developed 3 months after ICI therapy.

Results: A total of 36 patients with 3 CMRs (60.7±9.2 years old, 77.8% male) were included in the analysis. Left ventricular-global radial strain (LV-GRS) decreased significantly at the second follow-up (37.9%±8.5% *vs.* 33.1%±1.0%; P=0.014), but left ventricular ejection fraction (LVEF) did not change significantly (51.5%±6.0% *vs.* 49.2%±6.5%; P>0.05). A total of 7 patients (19.4%) had developed CTRCD by the second follow-up. Baseline clinical and CMR parameters did not differ between the CTRCD group and the non-CTRCD group (P>0.05 for all). In the CTRCD group, the left ventricular-global circumferential strains (LV-GCSs) showed significant reductions at both the first and second follow-up (P=0.008 and 0.035, respectively), but the LVEF only showed a significant reduction at the second follow-up (P<0.001). The relative reduction of LV-GRS at the second follow-up was significantly higher in the CTRCD group than in the non-CTRCD group (29.8%±25.8% *vs.* 6.8%±20.4%; P=0.036) and was used to predict CTRCD developed at the 3-month timepoint after ICI therapy [area under the curve (AUC) =0.759; P=0.036].

Conclusions: In the early stage of ICI therapy, assessment of myocardial strain can be used to detect subclinical left ventricular systolic dysfunction in patients with lung cancer earlier than LVEF. The relative reduction of LV-GRS can be used to predict CTRCD 3 months after ICI therapy.

Keywords: Immune checkpoint inhibitor (ICI); cardiotoxicity; cancer therapy-related cardiac dysfunction (CTRCD); cardiovascular magnetic resonance (CMR); myocardial strain

Submitted Jan 14, 2022. Accepted for publication Jul 17, 2022.
doi: 10.21037/qims-22-41
View this article at: https://dx.doi.org/10.21037/qims-22-41

Introduction

In recent years, immune checkpoint inhibitors (ICIs) have been increasingly applied in cancer therapy. Cardiotoxicity resulting from can present as myocarditis, arrhythmia, pericarditis, and cardiac dysfunction (1). Among these complications, ICI-related myocarditis is an uncommon but severe complication, with an incidence of less than 1.0% but a high mortality of 46% (2-4). The time of myocarditis after the initiation of ICIs varies greatly, ranging from 17 to 75 days (average =34 days), and about 81% of myocarditis cases are reported within 3 months after treatment (5-7). However, ICI-related cardiotoxicity can extend beyond myocarditis, and it is important to detect subclinical or mild myocardial injury (for example, asymptomatic left ventricular dysfunction), which may influence clinical decisions regarding the choice of ICI therapy, indication for cardio-protection, or frequency of surveillance.

Cardiovascular magnetic resonance (CMR) plays a crucial role in diagnosing and monitoring cardiotoxicity during cancer therapies, with advantages such as the ability to conduct non-invasive evaluation of cardiac function and tissue characterization in a single scan (8). Myocardial strain based on CMR tissue tracking is widely used to detect subclinical myocardial dysfunction and is thought to be a more sensitive diagnostic index than ejection fraction (9,10). Cardiovascular (CV) changes on CMR in patients receiving ICI therapy have been observed in some retrospective studies (11-13). To date, there has been only 1 prospective study describing the changes on CMR in patients receiving ICI treatment, the findings of which indicated that the usage of ICI may induce a high burden of subclinical myocardial injury, including myocardial inflammation and systolic dysfunction (14). As reported by Oikonomou *et al.* (15), assessment of myocardial strain can be used to detect subclinical cancer therapy-related cardiac dysfunction (CTRCD) in patients receiving cardiotoxic cancer therapy. Assessment of CMR parameters at baseline may facilitate appropriate interpretation of subsequent results/changes during regular monitoring. Accordingly, we performed a prospective, longitudinal cohort study to (I) dynamically assess and monitor subclinical cardiotoxicity in patients with lung cancer receiving ICI therapy and (II) explore if CMR parameters can help predict cardiotoxicity during the early stages of ICI therapy. We present the following article in accordance with the STARD reporting checklist (available at https://qims.amegroups.com/article/view/10.21037/qims-22-41/rc).

Methods

Study participants

From January 2021 to December 2021, patients with lung cancer in a chest tumor ward of the Cancer Center at Wuhan Union Hospital who were ready to receive ICI therapy were consecutively recruited. They were scheduled to undergo CMR and laboratory examinations at 3 timepoints: before (baseline), 3 weeks after (1st follow-up), and 3 months after (2nd follow-up) the initiation of ICI therapy, respectively. Demographics, CV risk factors, primary cancer type, and details of treatment were extracted from electronic medical records. The results of the laboratory examinations conducted at the same time as the CMR examinations were also recorded. The exclusion criteria for patients included: (I) failure to complete a CMR examination due to various reasons (e.g., poor breath-holding ability or an inability to lie down for a duration of approximately 40 min due to bone metastasis) and (II) treatment with left-side radiotherapy after the initiation of ICI therapy. Only patients who completed the entire study protocol were included in the final analysis. The study was conducted in accordance with the Declaration of Helsinki (as revised in 2013). This study was registered at the Chinese Clinical Trials Registry Center

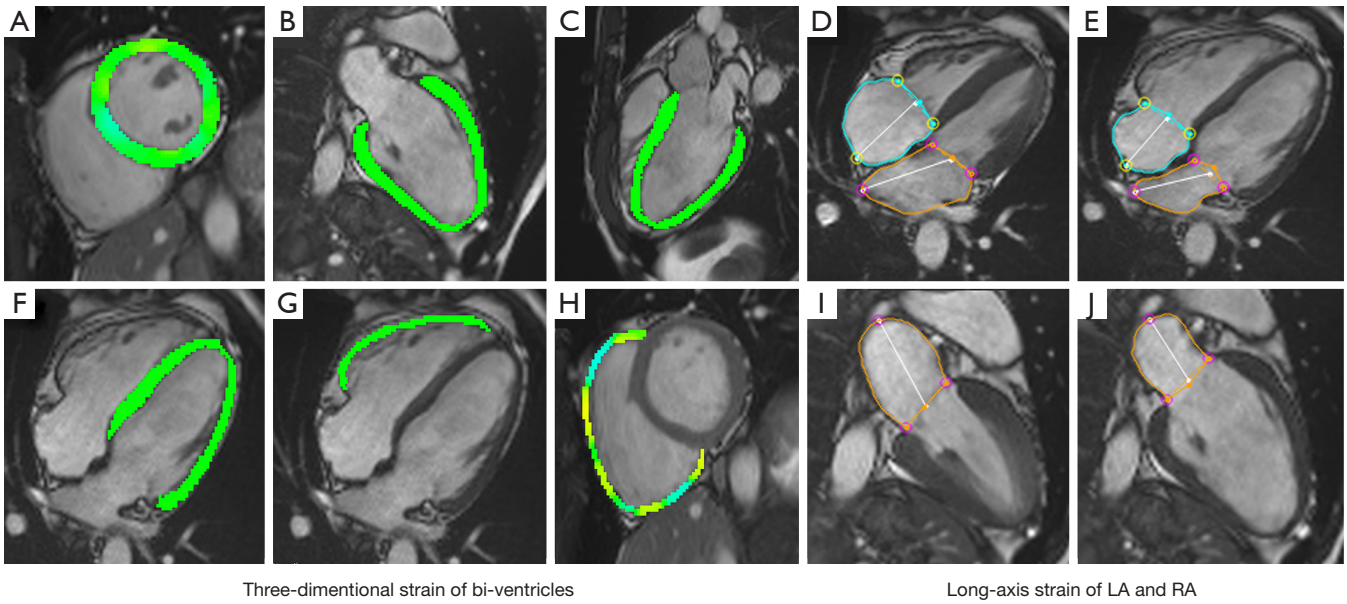

Figure 1 Strain analysis based on CMR tissue tracking. The LV strain is visualized by colored overlay on (A) short-axis and (B-D) 3 long-axis slices in the end-diastolic phase. The RV free wall strain is derived by contouring (E) 4-chamber long axis and (F) short-axis cine images. The contours of LA (orange line) and RA (blue line) at end-systolic and end-diastolic phases were automatically generated in (I,J) 2-chamber and (G,H) 4-chamber long-axis slices to calculate regional deformation, and the white lines connect the LA/RA apices and the midpoints of the mitral/tricuspid valves' connecting lines, respectively. LA, left atrium; RA, right atrium; CMR, cardiovascular magnetic resonance; LV, left ventricle; RV, right ventricle.

(http://www.chictr.org.cn/index.aspx; registration number ChiCTR2100041797), and was approved by the Ethics Committee of Tongji Medical College, Huazhong University of Science and Technology (No. [2019]S878). Written informed consent was provided by each participant.

CMR protocol

All CMR examinations were performed with a 1.5 T scanner (Magnetom Altea, Siemens Healthineers, Erlangen, Germany) using an 18-channel, cardiac phased-array receiver coil, electrocardiographic gating, and with breath-holding. A balanced steady-state free precession (bSSFP) sequence was used for cine acquisition, including a stack of short-axis slices covering the entire left ventricle (LV) and three long-axis slices (2-, 3-, and 4-chamber images). Native T1 mapping was performed in the 3 short-axis slices (basal, middle, and apical) using a Modified Look-Locker inversion recovery (MOLLI) sequence with a 5b(3b)3b sampling scheme. The T2 mapping was scanned using a T2-prepared, single-shot bSSFP sequence, with 3 different echo times: 0, 30, and 55 ms. Late gadolinium enhancement (LGE) was obtained at least 10 min after administering the contrast injection (0.2 mmol/kg, Magnevist; Bayer Healthcare, Leverkusen, Germany) in all short-axis planes and three long-axis planes, using a conventional two-dimensional (2D) phase sensitive inversion recovery (PSIR) sequence by breath holding appended by a motion-correction free-breathing PSIR sequence (to assist identification of LGE in patients with poor breath-holding ability). Post-contrast T1 mapping was acquired with the same planes of native T1 mapping after LGE scanning with a 4b(1b)3b(1b)2b sampling scheme.

CMR image analysis

Analyses of cardiac function and myocardial strain were performed using commercially available software (CVI 42 v. 5.13.5; Circle Cardiovascular Imaging, Inc., Calgary, Canada). Endocardial and epicardial borders of the LV and the right ventricle (RV) were automatically tracked and manually corrected in all cine sequences in both end-diastolic and end-systolic phases (*Figure 1*). Parameters of bi-ventricular end-diastolic volume, end-systolic volume, and stroke volume were normalized to body

surface area (BSA). The global radial strain (GRS), global circumferential strain (GCS), and global longitudinal strain (GLS) of the bi-ventricles were derived by the three-dimensional (3D) model of CVI software. Endocardial and epicardial borders of the left atrium (LA) and the right atrium (RA) were automatically evaluated by contouring the 2- and 4-chamber long-axis slices throughout the cardiac cycle in the long-axis strain analysis module of CVI software. The RA long-axis strain was obtained by a 4-chamber long-axis slice, and the average LA long-axis strain was obtained from both long-axis slices (*Figure 1*).

Native and post-contrast T1 values of both the myocardium and the blood pool were obtained by drawing the region of interest (ROI) on 3 short-axis slices in the CVI software. Blood samples for the determination of the hematocrit were taken on the day of the CMR scanning. The extracellular volume (ECV) value of the global myocardium was calculated from native and post-contrast T1 maps, as previously described (16). The presence, location, and pattern of LGE were visually evaluated by 2 independent radiologists (JL and YC) with 5 and 6 years of experience, respectively, in the CMR field. A final consensus was achieved by discussion.

Definitions of cardiotoxicity of ICI therapy

Cardiotoxicity of ICI therapy is defined as CTRCD with a relative left ventricular ejection fraction (LVEF) reduction of more than 10% to a value below 55% (17,18).

Statistical analysis

The normality of continuous variables was tested using the Shapiro-Wilk test. Continuous variables were described as mean ± standard deviation (SD) or median with interquartile range (IQR). Serial measurements based on CMR were compared using one-way repeated measures analysis of variance (RM-ANOVA). Categorical variables were presented with number and percentage and were compared using the chi-square test or Fisher's exact test. The relationships between changes in LVEF and changes in LV global strains were assessed by Pearson's or Spearman's correlation tests. Based on CTRCD observed at second follow-up, patients were divided into a CTRCD group and a non-CTRCD group. Continuous measurements of the CTRCD group and non-CTRCD group were compared using the independent sample *t*-test or Mann-Whitney U test, and categorical variables were compared using the chi-square test or Fisher's exact test. Receiver operating characteristic (ROC) analysis was performed to identify the ability of CMR parameters in predicting the development of CTRCD. The intra- and inter-observer agreements of CMR quantitative parameters were evaluated by the intraclass correlation coefficient (ICC), and an ICC >0.750 was considered high consistency. The baseline CMR images of 15 participants were analyzed by the same reader (YC) at 2 timepoints (2 weeks apart) and by a second, blinded reader (MY), respectively. Statistical analyses of all data were performed using SPSS software (version 22.0; IBM Corp., Armonk, NY, USA) and GraphPad Prism (version 9.0.0; GraphPad Software, Inc., San Diego, CA, USA). A 2-sided P value <0.05 was considered statistically significant.

Results

A total of 36 patients with 3 CMRs were included (60.7±9.2 years old; 77.8% male) (*Figure 2*). The median time between the initiation of ICI therapy and first and second follow-ups were 22 (IQR, 20 to 23) and 83 (IQR, 73 to 90) days, respectively.

Baseline clinical characteristics

All baseline clinical characteristics are presented in *Table 1*. There were 28 (77.8%) of the 36 patients with at least one CV risk factor. All participants (100%) received ICI monotherapy using anti-programmed death 1 (anti PD-1; including camrelizumab, sintilimab, tislelizumab, and pembrolizumab) or anti-programmed death-ligand 1 (anti PD-L1; including durvalumab and atezolizumab) therapy. There were 32 (88.9%) participants who received ICI therapy combined with chemotherapy as a first-line treatment method. None of the participants received anthracycline-based chemotherapy.

Results of laboratory and CMR parameters at baseline, first follow-up, and second follow-up

The results of laboratory and CMR parameters at three timepoints are summarized in *Table 2*. The results of the laboratory examinations did not change significantly after ICI therapy (P>0.05 for all), and none of the patients showed an abnormal high-sensitivity troponin (hs-TnI) value (>26.2 ng/L) during follow-up. After ICI therapy, LVEF progressively decreased, but there were no significant differences among the 3 CMRs (P>0.05). Left ventricular-global radial strain (LV-GRS) at the second follow-up

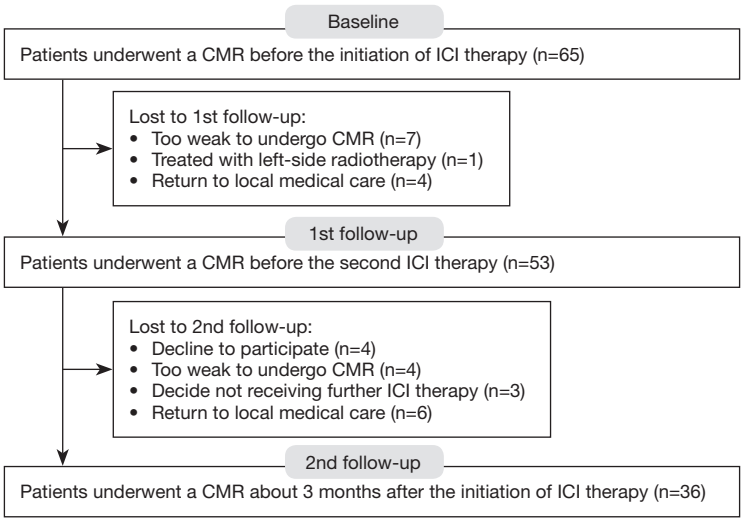

Figure 2 Flow chart of our study cohort. CMR, cardiovascular magnetic resonance; ICI, immune checkpoint inhibitor.

Table 1 A full summary of patient demographics

Demographics	Baseline (n=36)
Age (years)	60.7±9.2
Male gender	28 (77.8%)
CV risk factors	28 (77.8%)
BMI ≥25 (kg/m^2)	8 (22.2%)
Smoking	18 (50.0%)
Coronary artery disease	5 (13.9%)
Hypertension	11 (30.6%)
Diabetes mellitus	1 (2.8%)
Hyperlipidemia	6 (16.7%)
ICI regimen	
Dual therapy	0
Monotherapy	36 (100.0%)
Anti PD-1	30 (83.3%)
Anti PD-L1	6 (16.7%)
Anti CTLA-4	0
Concurrent treatment	
Chemotherapy/anthracyclines	32 (88.9%)/0

Values are mean ± SD or n (%). CV, cardiovascular; BMI, body mass index; ICI, immune checkpoint inhibitor; PD-1, programmed death 1; PD-L1, programmed death-ligand 1; CTLA-4, cytotoxic T-lymphocyte-associated protein 4; SD, standard deviation.

showed a significant difference compared with the baseline (37.9%±8.5% *vs.* 33.1%±1.0%; P=0.014). Right ventricular ejection fraction (RVEF) at the second follow-up revealed a significant reduction compared with the baseline and first follow-up (P=0.008 and 0.038, respectively). The right ventricular-global radial strain (RV-GRS) at both first and second follow-up showed significant differences compared with the baseline (P=0.027 and 0.001, respectively). Average LA long-axis strain and RA long-axis strain did not reveal significant differences among the 3 timepoints (P>0.05 for all). Regarding parameters of tissue characteristics, the native T1, post-contrast T1, ECV, and T2 values of the global myocardium showed no significant differences compared with the baseline (P>0.05).

Sub-epicardial enhancement at the inferior right ventricular insertion point (RVIP) was common, occurring in 5 patients (13.9%) at baseline. The number had slightly increased at the first (n=9, 25.0%) and second (n=10, 27.8%) follow-ups, but showed significant differences compared with the baseline (P=0.234 and 0.147, respectively). None of the patients were observed to have visible diffuse myocardial edema on the T2 stir sequence. The amount of pericardial effusion was found slightly increased in 1 patient (2.8%) at first follow-up and in 2 patients (5.6%) at second follow-up (*Figure 3*) compared with that found in patients at baseline.

Associations between changes in LVEF and changes in LV global strains

As shown in *Figure 4*, there were significant correlations

Table 2 The results of laboratory and CMR measurements at baseline, first follow-up, and second follow-up

Parameters	Baseline (n=36)	1st follow-up (n=36)	2nd follow-up (n=36)
Times of ICI therapy at follow-up, number	–	1	3 [3, 4]
Time interval since first ICI therapy, days	–	22 [20, 23]	83 [73, 90]
Laboratory results			
LDH (U/L)	193.0 [163.0, 263.0]	197.0 [158.0, 249.0]	188.0 [147.5, 249.0]
CK (U/L)	57.0 [38.0, 73.3]	51.0 [35.0, 70.0]	51.0 [37.0, 75.0]
CK-MB (ng/mL)	0.6 [0.3, 0.8]	0.5 [0.4, 0.7]	0.5 [0.3, 0.7]
hs-TnI (ng/L)	1.3 [0.9, 3.1]	1.9 [0.8, 3.3]	1.6 [1.0, 2.6]
CMR parameters			
LVEDVi (mL/m^2)	72.8±15.5	70.8±15.5	69.8±15.9
LVESVi (mL/m^2)	35.5±8.1	35.0±8.7	34.9±8.7
LVSVi (mL/m^2)	37.3±10.1	35.8±10.1	34.9±9.8
LVEF (%)	51.5±6.0	50.4±6.9	49.2±6.5
RVEDVi (mL/m^2)	68.0±15.3	67.7±15.6	67.2±18.0
RVESVi (mL/m^2)	37.0±10.3	37.8±9.3	39.2±9.2
RVSVi (mL/m^2)	31.0±9.0	29.9±9.2	28.0±11.2
RVEF (%)	46.5±8.1	43.9±8.5	40.3±9.4*#
LV-GRS (%)	37.9±8.5	36.1±9.7	33.1±1.0*
LV-GCS (%)	−18.0±2.8	−17.6±2.6	−17.7±2.9
LV-GLS (%)	−13.4±3.2	−13.2±3.1	−12.7±2.5
RV-GRS (%)	32.8±11.3	28.8±8.9*	25.8±8.7*
RV-GCS (%)	−12.1±4.0	−11.9±4.8	−11.7±4.3
RV-GLS (%)	−14.8±5.0	−14.6±5.4	−13.4±5.1
Average LA long-axis strain (%)	27.0±7.1	26.5±9.3	26.3±9.5
RA long-axis strain (%)	31.7±8.9	27.9±8.7	27.3±9.1
Native T1 (ms)	1,030.7±44.0	1,023.3±53.4	1,027.6±50.9
Post-contrast T1 (ms)	448.2±39.5	451.4±42.6	459.8±40.6
ECV (%)	28.5±3.3	29.0±4.6	28.4±3.7
T2 (ms)	46.3±3.8	46.2±5.4	47.8±5.4

Continuous variables were described as mean ± SD or median [IQR]. *, P<0.05 compared with baseline; #, P<0.05 compared with first follow-up. CMR, cardiovascular magnetic resonance; ICI, immune checkpoint inhibitor; LDH, lactate dehydrogenase; CK, creatine kinase; hs-TnI, high-sensitivity troponin I; LVEDVi, left ventricular end-diastolic volume index; LVESVi, left ventricular end-systolic volume index; LVSVi, left ventricular stroke volume index; LVEF, left ventricular ejection fraction; RVEDVi, right ventricular end-diastolic volume index; RVESVi, right ventricular end-systolic volume index; RVSVi, right ventricular stroke volume index; RVEF, right ventricular ejection fraction; LV-GRS, left ventricular global radial strain; LV-GCS, left ventricular global circumferential strain; LV-GLS, left ventricular global longitudinal strain; RV-GRS, right ventricular global radial strain; RV-GCS, right ventricular global circumferential strain; RV-GLS, right ventricular global longitudinal strain; LA, left atrium; RA, right atrium; ECV, extracellular volume; SD, standard deviation; IQR, interquartile range.

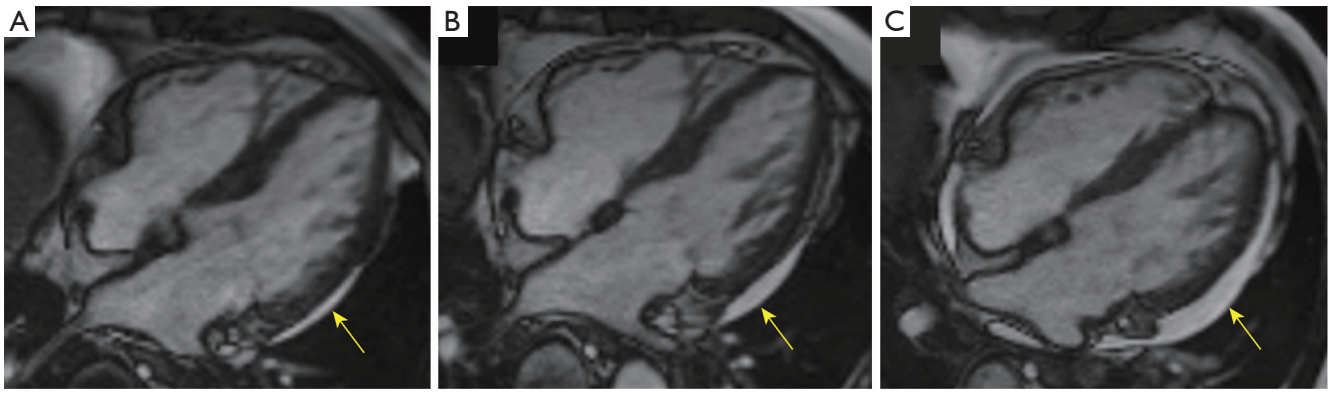

Figure 3 A 66-year-old male patient was observed with pericardial effusion (arrows) on CMRs at 3 timepoints. Compared with (A) baseline, the pericardial effusion revealed a slight increase at (B) first follow-up and (C) second follow-up. CMR, cardiovascular magnetic resonance.

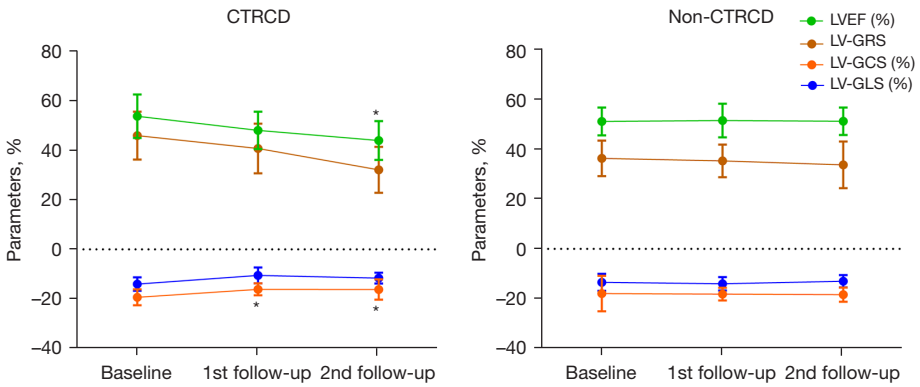

Figure 4 LVEF and global strain values at 3 timepoints in the CTRCD group and non-CTRCD group. *, P<0.05 compared with baseline value. CTRCD, cancer therapy-related cardiac dysfunction; LVEF, left ventricular ejection fraction; LV-GRS, left ventricular-global radial strain; LV-GCS, left ventricular-global circumferential strain; LV-GLS, left ventricular-global longitudinal strain.

between changes in LVEF and changes in LV global strains at 2 time-points (compared with baseline) during follow-up (P<0.05 for all).

Comparison of clinical and CMR parameters in the CTRCD group and the non-CTRCD group

A total of 7 patients (19.4%) had developed CTRCD by the second follow-up. Among them, 2 patients (5.6%) met CTRCD criteria at first follow-up. We further divided the patients into a CTRCD group (n=7) and a non-CTRCD group (n=29) at the second follow-up, and compared the baseline clinical and CMR parameters between these subgroups (*Table 3*). The combined CV risk factors and results of baseline laboratory examinations did not differ between the CTRCD group and the non-CTRCD group (P>0.05 for all). There were no significant differences in baseline LVEF between the CTRCD group and the non-CTRCD group (53.4%±8.7% *vs.* 51.1%±5.3%; P=0.253). As shown in *Figure 5*, the LVEF of patients in the CTRCD group had decreased significantly at the second follow-up (P<0.001). The absolute values of the left ventricular-global circumferential strain (LV-GCS) decreased significantly at both timepoints of follow-up compared with the baseline (P=0.008 and 0.035, respectively).

We also compared the relative reductions of LVEF and global strains at the second follow-up in the CTRCD group and non-CTRCD group (*Figure 6*). The relative reduction of both LVEF (18.1%±5.3% *vs.* 1.8%±5.8%; P<0.001) and LV-GRS (29.8%±25.8% *vs.* 6.8%±20.4%; P=0.036) differed

Table 3 Baseline clinical and CMR parameters in the CTRCD and non-CTRCD groups

Parameters	CTRCD (n=7)	Non-CTRCD (n=29)	P value
Age (years)	61.4±6.1	60.5±9.9	0.969
Male gender	6 (85.7)	23 (79.3)	1.000
BMI ≥25 kg/m^2	2 (28.6)	6 (20.7)	1.000
Smoking	3 (42.9)	15 (51.7)	1.000
Coronary artery disease	1 (14.3)	4 (13.8)	1.000
Hypertension	1 (14.3)	10 (34.5)	0.559
Diabetes mellitus	0	1 (3.4)	1.000
Hyperlipidemia	1 (14.3)	5 (17.2)	1.000
Number of CV risk factors	1 [1, 1]	1 [1, 2]	0.450
Combined with chemotherapy	6 (85.7)	20 (69.0)	0.676
Anti PD-1	5 (71.4)	24 (82.8)	0.883
Times of ICI therapy	3 [3, 3]	3 [3, 4]	0.537
Baseline LDH (U/L)	263.0 [184.0, 277.0]	192.0 [161.0, 230.0]	0.270
Baseline CK (U/L)	67.0 [38.0, 92.0]	53.5 [38.3, 72.8]	0.384
Baseline CK-MB (ng/mL)	0.5 [0.3, 1.0]	0.6 [0.3, 0.8]	0.901
Baseline hs-TnI (ng/L)	1.0 [0.8, 4.3]	1.3 [0.9, 3.1]	0.739
Baseline LVEF (%)	53.4±8.7	51.1±5.3	0.253
Baseline LV-GRS (%)	41.4±5.6	37.1±6.2	0.106
Baseline LV-GCS (%)	−19.2±3.2	−17.8±2.7	0.241
Baseline LV-GLS (%)	−13.9±2.7	−13.3±3.4	0.681
Baseline native T1 (ms)	1,028.3±43.0	1,031.3±44.9	0.876
Baseline post-contrast T1 (ms)	446.9±33.0	448.5±41.4	0.924
Baseline ECV (%)	27.5±2.3	28.8±3.5	0.373
Baseline T2 (ms)	44.3±1.8	46.8±4.0	0.117

Variables were described as mean ± SD, median (IQR) or n (%). CMR, cardiovascular magnetic resonance; CTRCD, cancer therapy-related cardiac dysfunction; BMI, body mass index; CV, cardiovascular; PD-1, programmed death 1; ICI, immune checkpoint inhibitor; LDH, lactate dehydrogenase; CK, creatine kinase; hs-TnI, high-sensitivity troponin I; LVEF, left ventricular ejection fraction; LV-GRS, left ventricular-global radial strain; LV-GCS, left ventricular-global circumferential strain; LV-GLS, left ventricular-global longitudinal strain; ECV, extracellular volume; SD, standard deviation; IQR, interquartile range.

between the CTRCD group and the non-CTRCD group. Furthermore, the ROC analysis revealed that the relative reduction of LV-GRS can predict CTRCD after ICI therapy at second follow-up with an area under the curve (AUC) of 0.759 (*Table 4*).

Inter- and intra-observer reproducibility

Intra- and inter-observer agreements are shown in *Table 5*. Except for RV-GRS, other CMR quantitative parameters showed good intra- and inter-observer agreements, with ICC values >0.750.

Discussion

We conducted a prospective, longitudinal study of lung cancer patients receiving ICI therapy. Assessment of LV-GRS can be used to detect subclinical systolic dysfunction

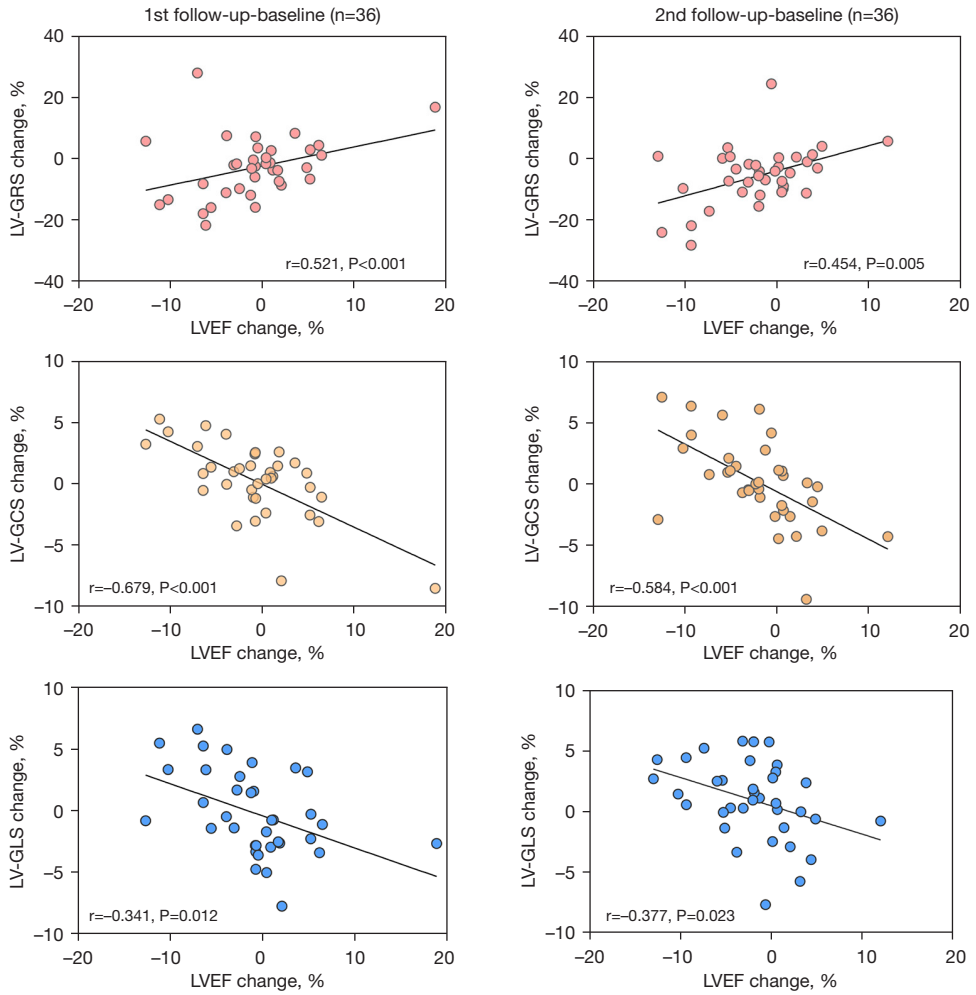

Figure 5 Correlation between changes in LVEF values and changes in LV global strain values during follow-up. LV-GRS, left ventricular-global radial strain; LV-GCS, left ventricular-global circumferential strain; LV-GLS, left ventricular-global longitudinal strain; LVEF, left ventricular ejection fraction; LV, left ventricle.

of LV at the early stage of ICI therapy. In patients who developed CTRCD 3 months after ICI therapy, LV-GCS decreased before LVEF, and the relative reduction of LV-GRS provided the ability to predict the CTRCD that developed at the 3-month timepoint after ICI therapy.

Cardiac dysfunction is a long-established adverse effect in patients receiving cancer therapy, and it has been reported in patients receiving ICI therapy (19). The baseline LVEF value in our study was lower than that in a another CMR study conducted by Faron *et al.*, but was similar to that in the CMR study conducted by Higgins *et al.* (14,20). We speculated that this may be due to the baseline characteristics of the patient cohort in our study [with lung cancer, older age (60.7±9.2 years old), and a large proportion (77.8%) of patients with at least 1 CV risk factor]. Subclinical cardiac dysfunction is reported to have an association with pulmonary function, and smoking is also an independent risk factor for worse RV function (21,22). In patients with lung cancer (especially at the advanced stage), a history of prior cancer therapy may have impacted the LVEF value detected at the baseline in this study. In the present study, none of the patients showed typical clinical symptoms of cardiac failure. Given that subclinical or mild cardiac dysfunction may have symptoms overlapping with lung cancer, the CMR manifestations observed were thought to mainly present as the subclinical cardiotoxicity of ICI therapy.

In a CMR study, LV-GRS and LV-GLS were observed

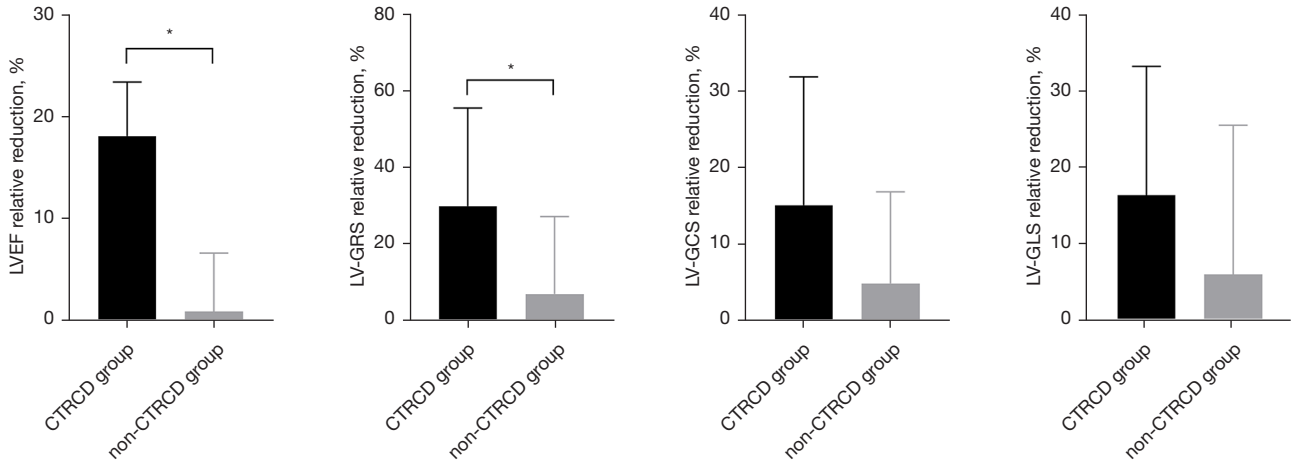

Figure 6 Comparison of relative reductions of LVEF and global strains in the CTRCD group and non-CTRCD group 3 months after ICI therapy. *, P<0.05. LVEF, left ventricular ejection fraction; CTRCD, cancer therapy-related cardiac dysfunction; LV-GRS, left ventricular-global radial strain; LV-GCS, left ventricular-global circumferential strain; LV-GLS, left ventricular-global longitudinal strain; ICI, immune checkpoint inhibitor.

Table 4 ROC analysis of left ventricular global strain relative reductions and the prediction of CTRCD at second follow-up

Parameters	Sensitivity (%)	Specificity (%)	Cut-off value (%)	AUC	P value
LV-GRS relative reduction	71.4	82.76	22.6	0.759	0.036*
LV-GCS relative reduction	71.4	75.9	9.5	0.714	0.082
LV-GLS relative reduction	57.1	77.8	21.2	0.651	0.225

*, P<0.05. ROC, receiver operating characteristic; CTRCD, cancer therapy-related cardiac dysfunction; AUC, area under the curve; LV-GRS, left ventricular-global radial strain; LV-GCS, left ventricular-global circumferential strain; LV-GLS, left ventricular-global longitudinal strain.

to decrease in patients with ICI-related myocarditis with preserved LVEF (20). In our study, we observed a significant reduced LV-GRS at the second follow-up, but the LVEF did not show a significant change compared with the baseline. The animal model study found that the GRS was decreased by 51% in anti PD-1-treated, tumor-bearing mice as a sign for globally impaired LV contractility (23). A mathematical model proposed by MacIver *et al*. (24) indicated that LVEF is determined by both myocardial strain and wall thickness, and the model explained why reduced myocardial strain may be observed in patients with normal LVEF values. The mechanism of cardiotoxicity using ICI therapy is not fully understood. In clinical contexts, patients with lung cancer mainly receive anti PD-1/PD-L1 therapy. The greatest proportion of cardiac PD-L1 is located on cardiac endothelial cells, and at the early stage of ICI therapy, LV dysfunction may be associated with disrupted immune homeostasis and induced dysregulated metabolism (24). PD-L1 expression in the myocardium is upregulated in the situation of cardiac stress, including ischemia-reperfusion and left ventricular hypertrophy in preclinical models (25). The cardiotoxicity of ICI therapy can be represented in different forms and severity levels, and only a small portion of patients manifest severe cardiotoxicity including myocarditis, which requires immediate treatment. Those cardiotoxic effects which develop more slowly may have equally important detrimental effects.

In our study, 7 patients (19.4%) met the CTRCD criteria at the second follow-up (3 months) after ICI therapy. In patients who developed CTRCD (n=7), LV-GCS decreased before LVEF after ICI therapy. As we mentioned above, in the whole patient cohort (n=36), LV-GRS was more sensitive than LVEF in detecting systolic dysfunction after ICI therapy. These findings illustrated

Table 5 Inter- and intra-observer agreements of CMR parameters

Parameters	Intra-observer		Inter-observer	
	ICC	95% CI	ICC	95% CI
LV-GRS	0.925	0.842–0.964	0.906	0.795–0.958
LV-GCS	0.960	0.905–0.979	0.973	0.882–0.980
LV-GLS	0.958	0.878–0.986	0.947	0.866–0.978
RV-GRS	0.658	0.557–0.750	0.625	0.502–0.768
RV-GCS	0.885	0.754–0.947	0.859	0.732–0.938
RV-GLS	0.780	0.645–0.824	0.756	0.625–0.835
Average LA long-axis strain	0.934	0.820–0.967	0.923	0.799–0.955
RA long-axis strain	0.953	0.886–0.974	0.945	0.858–0.978
Native T1	0.985	0.893–0.995	0.978	0.870–0.985
Post-contrast T1	0.970	0.905–0.998	0.954	0.877–0.989
T2	0.969	0.887–0.985	0.972	0.895–0.995

CMR, cardiovascular magnetic resonance; ICC, intraclass correlation coefficient; CI, confidence interval; LV-GRS, left ventricular global radial strain; LV-GCS, left ventricular global circumferential strain; LV-GLS, left ventricular global longitudinal strain; RV-GRS, right ventricular global radial strain; RV-GCS, right ventricular global circumferential strain; RV-GLS, right ventricular global longitudinal strain; LA, left atrium; RA, right atrium.

the importance of myocardial strain in detecting systolic dysfunction. It is unknown if this denoted the chronological order of impairment strain parameters impairment, and more longitudinal studies are still needed to clarify this theory. Meanwhile, this raised a question that the specific values of LVEF or global strains may not fully reflect the influence of ICI therapy in an individual patient, and new cardiac dysfunction compared with the baseline may help identify ICI-related cardiotoxicity. In our study, the changes in LVEF were significantly correlated with changes in global strain values. This phenomenon was consistent with findings of previous studies (26,27). At the time of the second follow-up, we further compared the relative reductions of LV global strain values between the CTRCD group and the non-CTRCD group. The relative reduction of LV-GRS observed in the CTRCD group was higher than that in the non-CTRCD group and had a predictive value in identifying the CTRCD population at the early stage of ICI therapy (3 months). The value of LV strain in predicting cardiotoxicity in patients receiving cancer therapy has been confirmed (28). It is very important to explore the feasibility of CMR indexes in predicting the development of cardiotoxicity before starting or during the cancer therapy. In addition, the early detection of subclinical cardiotoxicity is crucial in the effort to prevent irreversible cardiac injury. In a previous report, some CV support drugs, such as angiotensin-converting enzyme inhibitor/angiotensin receptor blocker and beta blockers, have been shown to prevent CTRCD in patients receiving anthracyclines-based chemotherapy (29). However, the evidence and strength of recommendations for the management of ICI-related cardiotoxicity is preliminary and relatively scant in practical detail. Currently, ICI-related cardiotoxicity remains therapeutically challenging, and there is a lack of hard evidence to support these therapeutic strategies. There is a need to explore the appropriate cardioprotective therapeutic strategies in subclinical patients developing CTRCD.

Assessment of RV function has been included in the CV evaluation in our study. Grover *et al*. found a significant decrease in RVEF during anthracycline and/or trastuzumab therapy, which emphasized the need for bi-ventricular function assessment of CTRCD (30). In our patient cohort, RVEF decreased significantly at the 3-month timepoint after ICI therapy, and RV-GRS decreased before RVEF after ICI therapy. The prognostic value of the concomitant reduction of bi-ventricular strains will be further studied after expanding the sample size of our patient cohort. The LA long-axis strain was reported to be reduced in patients with confirmed myocarditis, which was associated with LV diastolic dysfunction (31). In our study, the long-axis strain

of LA and RA did not decrease significantly compared with the baseline, which may indicate that the diastolic functions of the ventricles were not impaired after ICI therapy.

Another important strength of CMR is its ability to provide tissue characterization techniques. The presence of LGE at RVIP (RVIP-LGE) has been reported in a retrospective study on patients with confirmed ICI-related myocarditis (20). The RVIP-LGE may be caused by an expanded extracellular space due to an exaggeration of the myocardial disarray and plexiform fibrosis at the RV and LV cross (32,33). It is reported that the presence of RVIP-LGE does not convey a worse prognosis in patients without other CMR evidence of myocardial injury (34). In our study, the number of patients with RVIP-LGE was observed to be slightly increased after ICI therapy but with no significance difference. The prospective study conducted by Faron *et al.* (14) also revealed no statistically significant increase of quantitative LGE at follow-up. The pattern of LGE in confirmed ICI-related myocarditis can appear as sub-epicardial or diffuse enhancement, but the presence of LGE showed low relevance with myocarditis (11). Therefore, the traditional criteria for diagnosing myocarditis are not always present in this disorder. We speculated that the pattern of RVIP-LGE should be analyzed by combining the clinical presentation with other supporting evidence. The clinical significance of this enhancement pattern and the manifestations of CMR-LGE in patients receiving ICI therapy need to be further explored.

A CMR study demonstrated that T1 mapping can provide important diagnostic value and prognostic value in patients with ICI-related myocarditis (35). Therefore, ICI-related cardiotoxicity may not be limited to rare side effects like myocarditis, and some more global and subclinical effects should raise attention (23). In this study that mainly focused on subclinical cardiotoxicity, T1, T2, and ECV values of global myocardium at follow-up showed no significant differences compared with baseline values. Patients receiving combination ICI therapy or anti-cytotoxic T lymphocyte-associated antigen 4 (CTLA-4) are more likely to experience ICI-related myocarditis (36). This may be due to there being no positive CMR clues regarding ICI-related myocarditis (increased level of tissue characteristics parameters) in the current study. The biomarkers (especially hs-TnI, which represents acute myocardial injury) did not exceed the normal range during this 3-month follow-up. We speculated that, in the early stage, the subclinical manifestations of myocardial fibrosis or inflammation were mild or still limited to a local region of the myocardium, rather than being diffusely spread. Secondly, the positive presentation of myocardial fibrosis/inflammation on CMR may be the result of a long-term consequence of constantly developing myocardial inflammation. On this occasion, it may be helpful to continuously monitor for inflammation or fibrosis in T1 or T2 mapping analyses. Pericardial effusion after ICI therapy has been reported in patients with lung cancer (37). However, it is more likely to be caused by disease progression if there is concomitant increased amounts of pericardial effusion and pleural effusion. The presence and increase of pericardial effusion need to be evaluated individually and determined whether their cause is ICI therapy.

Limitations

First, this was a single-center study with a small sample size and a single type of primary tumor. Second, as the baseline level of biomarkers did not differ between the CTRCD and the non-CTRCD groups and were limited to the study sample size and research period, none of the patients showed an abnormal level of hs-TnI (>26.2 ng/L). Therefore, the prognostic value of biomarkers in predicting cardiotoxicity assessed by CMR needs to be further studied. Third, most participants with lung cancer received chemotherapy (not anthracycline-based chemotherapy) as combined treatment method, and the CV effect of chemotherapy cannot be completely ignored. Therefore, the manifestations and the prognostic significance of CMR in patients receiving ICI therapy with different cancer types should be verified in further studies using larger cohort or multi-center results.

Conclusions

This prospective, longitudinal study using CMR showed that assessment of myocardial strain can be used to detect subclinical LV systolic dysfunction earlier than LVEF in the early stage of ICI therapy (within 3 months). A relative reduction of LV-GRS can predict the CTRCD developed 3 months after ICI therapy.

Acknowledgments

Funding: This study received funding support from the Fundamental Research Funds for the Central Universities (No. 2021yjsCXCY107), National Natural Science Foundation of China (No. 82071921), the clinic research

fund of Union Hospital (No. 2021xhlcj08), and Hubei Province Health Commission General Foundation of China (No. WJ2019M165).

Footnote

Reporting Checklist: The authors have completed the STARD reporting checklist. Available at https://qims.amegroups.com/article/view/10.21037/qims-22-41/rc

Conflicts of Interest: All authors have completed the ICMJE uniform disclosure form (available at https://qims.amegroups.com/article/view/10.21037/qims-22-41/coif). XZ is employed by Siemens Healthineers Ltd. The other authors have no conflicts of interest to declare.

Ethical Statement: The authors are accountable for all aspects of the work in ensuring that questions related to the accuracy or integrity of any part of the work are appropriately investigated and resolved. The study was conducted in accordance with the Declaration of Helsinki (as revised in 2013). The study was approved by the Ethics Committee of Tongji Medical College, Huazhong University of Science and Technology (No. [2019]S878), and written informed consent was obtained from each participant.

References

1. Lyon AR, Yousaf N, Battisti NML, Moslehi J, Larkin J. Immune checkpoint inhibitors and cardiovascular toxicity. Lancet Oncol 2018;19:e447-58.
2. Nghiem PT, Bhatia S, Lipson EJ, Kudchadkar RR, Miller NJ, Annamalai L, et al. PD-1 Blockade with Pembrolizumab in Advanced Merkel-Cell Carcinoma. N Engl J Med 2016;374:2542-52.
3. Johnson DB, Balko JM, Compton ML, Chalkias S, Gorham J, Xu Y, et al. Fulminant Myocarditis with Combination Immune Checkpoint Blockade. N Engl J Med 2016;375:1749-55.
4. Johnson DB, Reynolds KL, Sullivan RJ, Balko JM, Patrinely JR, Cappelli LC, Naidoo J, Moslehi JJ. Immune checkpoint inhibitor toxicities: systems-based approaches to improve patient care and research. Lancet Oncol 2020;21:e398-404.
5. Mahmood SS, Fradley MG, Cohen JV, Nohria A, Reynolds KL, Heinzerling LM, Sullivan RJ, Damrongwatanasuk R, Chen CL, Gupta D, Kirchberger MC, Awadalla M, Hassan MZO, Moslehi JJ, Shah SP, Ganatra S, Thavendiranathan P, Lawrence DP, Groarke JD, Neilan TG. Myocarditis in Patients Treated With Immune Checkpoint Inhibitors. J Am Coll Cardiol 2018;71:1755-64.
6. Porter DL, Levine BL, Kalos M, Bagg A, June CH. Chimeric antigen receptor-modified T cells in chronic lymphoid leukemia. N Engl J Med 2011;365:725-33.
7. Moslehi JJ, Salem JE, Sosman JA, Lebrun-Vignes B, Johnson DB. Increased reporting of fatal immune checkpoint inhibitor-associated myocarditis. Lancet 2018;391:933.
8. Saunderson CED, Plein S, Manisty CH. Role of cardiovascular magnetic resonance imaging in cardio-oncology. Eur Heart J Cardiovasc Imaging 2021;22:383-96.
9. Liu J, Li J, Pu H, He W, Zhou X, Tong N, Peng L. Cardiac remodeling and subclinical left ventricular dysfunction in adults with uncomplicated obesity: a cardiovascular magnetic resonance study. Quant Imaging Med Surg 2022;12:2035-50.
10. Qu YY, Paul J, Li H, Ma GS, Buckert D, Rasche V. Left ventricular myocardial strain quantification with two- and three-dimensional cardiovascular magnetic resonance based tissue tracking. Quant Imaging Med Surg 2021;11:1421-36.
11. Zhang L, Awadalla M, Mahmood SS, Nohria A, Hassan MZO, Thuny F, et al. Cardiovascular magnetic resonance in immune checkpoint inhibitor-associated myocarditis. Eur Heart J 2020;41:1733-43.
12. Escudier M, Cautela J, Malissen N, Ancedy Y, Orabona M, Pinto J, Monestier S, Grob JJ, Scemama U, Jacquier A, Lalevee N, Barraud J, Peyrol M, Laine M, Bonello L, Paganelli F, Cohen A, Barlesi F, Ederhy S, Thuny F. Clinical Features, Management, and Outcomes of Immune Checkpoint Inhibitor-Related Cardiotoxicity. Circulation 2017;136:2085-7.
13. Ganatra S, Neilan TG. Immune Checkpoint Inhibitor-Associated Myocarditis. Oncologist 2018;23:879-86.
14. Faron A, Isaak A, Mesropyan N, Reinert M, Schwab K,

Sirokay J, Sprinkart AM, Bauernfeind FG, Dabir D, Pieper CC, Heine A, Kuetting D, Attenberger U, Landsberg J, Luetkens JA. Cardiac MRI Depicts Immune Checkpoint Inhibitor-induced Myocarditis: A Prospective Study. Radiology 2021;301:602-9.
15. Oikonomou EK, Kokkinidis DG, Kampaktsis PN, Amir EA, Marwick TH, Gupta D, Thavendiranathan P. Assessment of Prognostic Value of Left Ventricular Global Longitudinal Strain for Early Prediction of Chemotherapy-Induced Cardiotoxicity: A Systematic Review and Meta-analysis. JAMA Cardiol 2019;4:1007-18.
16. Flett AS, Hayward MP, Ashworth MT, Hansen MS, Taylor AM, Elliott PM, McGregor C, Moon JC. Equilibrium contrast cardiovascular magnetic resonance for the measurement of diffuse myocardial fibrosis: preliminary validation in humans. Circulation 2010;122:138-44.
17. Zamorano JL, Lancellotti P, Rodriguez Muñoz D, Aboyans V, Asteggiano R, Galderisi M, Habib G, Lenihan DJ, Lip GYH, Lyon AR, Lopez Fernandez T, Mohty D, Piepoli MF, Tamargo J, Torbicki A, Suter TM; ESC Scientific Document Group. 2016 ESC Position Paper on cancer treatments and cardiovascular toxicity developed under the auspices of the ESC Committee for Practice Guidelines: The Task Force for cancer treatments and cardiovascular toxicity of the European Society of Cardiology (ESC). Eur Heart J 2016;37:2768-801.
18. Lambert J, Lamacie M, Thampinathan B, Altaha MA, Esmaeilzadeh M, Nolan M, Fresno CU, Somerset E, Amir E, Marwick TH, Wintersperger BJ, Thavendiranathan P. Variability in echocardiography and MRI for detection of cancer therapy cardiotoxicity. Heart 2020;106:817-23.
19. Peleg Hasson S, Arnold J, Merdler I, Sivan A, Shamai S, Geva R, Merimsky O, Shachar E, Waissengrin B, Moshkovits Y, Arbel Y, Topilsky Y, Rozenbaum Z, Wolf I, Laufer-Perl M. Cancer Therapeutics-related Cardiac Dysfunction in Patients Treated With Immune Checkpoint Inhibitors: An Understudied Manifestation. J Immunother 2021;44:179-84.
20. Higgins AY, Arbune A, Soufer A, Ragheb E, Kwan JM, Lamy J, Henry M, Cuomo JR, Charifa A, Gallegos C, Hull S, Coviello JS, Bader AS, Peters DC, Huber S, Mojibian HR, Sinusas AJ, Kluger H, Baldassarre LA. Left ventricular myocardial strain and tissue characterization by cardiac magnetic resonance imaging in immune checkpoint inhibitor associated cardiotoxicity. PLoS One 2021;16:e0246764.
21. von Krüchten R, Lorbeer R, Schuppert C, Storz C, Mujaj B, Schulz H, Kauczor HU, Peters A, Bamberg F, Karrasch S, Schlett CL. Subclinical cardiac impairment relates to traditional pulmonary function test parameters and lung volume as derived from whole-body MRI in a population-based cohort study. Sci Rep 2021;11:16173.
22. Moreira HT, Armstrong AC, Nwabuo CC, Vasconcellos HD, Schmidt A, Sharma RK, Ambale-Venkatesh B, Ostovaneh MR, Kiefe CI, Lewis CE, Schreiner PJ, Sidney S, Ogunyankin KO, Gidding SS, Lima JAC. Association of smoking and right ventricular function in middle age: CARDIA study. Open Heart 2020;7:e001270.
23. Michel L, Helfrich I, Hendgen-Cotta UB, Mincu RI, Korste S, Mrotzek SM, et al. Targeting early stages of cardiotoxicity from anti-PD1 immune checkpoint inhibitor therapy. Eur Heart J 2022;43:316-29.
24. MacIver DH, Adeniran I, Zhang H. Left ventricular ejection fraction is determined by both global myocardial strain and wall thickness. Int J Cardiol Heart Vasc 2015;7:113-8.
25. Baban B, Liu JY, Qin X, Weintraub NL, Mozaffari MS. Upregulation of Programmed Death-1 and Its Ligand in Cardiac Injury Models: Interaction with GADD153. PLoS One 2015;10:e0124059.
26. Ong G, Brezden-Masley C, Dhir V, Deva DP, Chan KKW, Chow CM, Thavendiranathan D, Haq R, Barfett JJ, Petrella TM, Connelly KA, Yan AT. Myocardial strain imaging by cardiac magnetic resonance for detection of subclinical myocardial dysfunction in breast cancer patients receiving trastuzumab and chemotherapy. Int J Cardiol 2018;261:228-33.
27. Jolly MP, Jordan JH, Meléndez GC, McNeal GR, D'Agostino RB Jr, Hundley WG. Automated assessments of circumferential strain from cine CMR correlate with LVEF declines in cancer patients early after receipt of cardio-toxic chemotherapy. J Cardiovasc Magn Reson 2017;19:59.
28. Giusca S, Korosoglou G, Montenbruck M, Geršak B, Schwarz AK, Esch S, Kelle S, Wülfing P, Dent S, Lenihan D, Steen H. Multiparametric Early Detection and Prediction of Cardiotoxicity Using Myocardial Strain, T1 and T2 Mapping, and Biochemical Markers: A Longitudinal Cardiac Resonance Imaging Study During 2 Years of Follow-Up. Circ Cardiovasc Imaging 2021;14:e012459.
29. Curigliano G, Lenihan D, Fradley M, Ganatra S, Barac A, Blaes A, et al. Management of cardiac disease in cancer patients throughout oncological treatment: ESMO consensus recommendations. Ann Oncol 2020;31:171-90.
30. Grover S, Leong DP, Chakrabarty A, Joerg L, Kotasek

D, Cheong K, Joshi R, Joseph MX, DePasquale C, Koczwara B, Selvanayagam JB. Left and right ventricular effects of anthracycline and trastuzumab chemotherapy: a prospective study using novel cardiac imaging and biochemical markers. Int J Cardiol 2013;168:5465-7.
31. Doerner J, Bunck AC, Michels G, Maintz D, Baeßler B. Incremental value of cardiovascular magnetic resonance feature tracking derived atrial and ventricular strain parameters in a comprehensive approach for the diagnosis of acute myocarditis. Eur J Radiol 2018;104:120-8.
32. Noureldin RA, Liu S, Nacif MS, Judge DP, Halushka MK, Abraham TP, Ho C, Bluemke DA. The diagnosis of hypertrophic cardiomyopathy by cardiovascular magnetic resonance. J Cardiovasc Magn Reson 2012;14:17.
33. Bradlow WM, Assomull R, Kilner PJ, Gibbs JS, Sheppard MN, Mohiaddin RH. Understanding late gadolinium enhancement in pulmonary hypertension. Circ Cardiovasc Imaging 2010;3:501-3.
34. Grigoratos C, Pantano A, Meschisi M, Gaeta R, Ait-Ali L, Barison A, Todiere G, Festa P, Sinagra G, Aquaro GD. Clinical importance of late gadolinium enhancement at right ventricular insertion points in otherwise normal hearts. Int J Cardiovasc Imaging 2020;36:913-20.
35. Thavendiranathan P, Zhang L, Zafar A, Drobni ZD, Mahmood SS, Cabral M, et al. Myocardial T1 and T2 Mapping by Magnetic Resonance in Patients With Immune Checkpoint Inhibitor-Associated Myocarditis. J Am Coll Cardiol 2021;77:1503-16.
36. Salem JE, Manouchehri A, Moey M, Lebrun-Vignes B, Bastarache L, Pariente A, Gobert A, Spano JP, Balko JM, Bonaca MP, Roden DM, Johnson DB, Moslehi JJ. Cardiovascular toxicities associated with immune checkpoint inhibitors: an observational, retrospective, pharmacovigilance study. Lancet Oncol 2018;19:1579-89.
37. Canale ML, Camerini A, Casolo G, Lilli A, Bisceglia I, Parrini I, Lestuzzi C, Del Meglio J, Puccetti C, Camerini L, Amoroso D, Maurea N. Incidence of Pericardial Effusion in Patients with Advanced Non-Small Cell Lung Cancer Receiving Immunotherapy. Adv Ther 2020;37:3178-84.

Cite this article as: Liu J, Cao Y, Zhu K, Yao S, Yuan M, Kong X, Liu X, Li Y, Cui Y, Han X, Zhou X, Meng R, Shi H. Early evaluation of subclinical cardiotoxicity in patients with lung cancer receiving immune checkpoint inhibitors by cardiovascular magnetic resonance: a prospective observational study. Quant Imaging Med Surg 2022;12(10):4771-4785. doi: 10.21037/qims-22-41

